

An analytic nonlinear model of thermo-poro-elastic pressure transients in porous rocks with application to deep CO₂ storage

Roman Kanivetsky¹, Ettore Salusti^{*,2,3}

⁽¹⁾ Department of Bioproducts and Biosystems Engineering, University of Minnesota, 1390 Eckles Ave, St. Paul, MN 55108, USA

⁽²⁾ ISMAR-CNR, Via Fosso del Cavaliere 100, Roma, 00147, Italy

⁽³⁾ INFN, sezione Roma 1, Università La Sapienza, Italy

Article history: received May 25, 2021; accepted September 23, 2021

Abstract

Today a CO₂ storage/sequestration is an important option for a significant enhancing of CO₂ sinks, to reduce the net carbon emissions into our planet atmosphere. Such storage/sequestration is a complex process, dealing with many facets of decision about the site selection, taking into consideration the local geological, geothermal, hydrodynamic and hydrocarbon potentials. In such multifaceted context, a thermo-poro-elastic nonlinear analytic model of fluid pressure P in deep rocks, can play an important role. To analyse these dynamics we here focus on the role of the matrix convection, on thermal dynamics and fluid/rock “frictions”. In addition we here show that pressure dynamics, induced by an eventual external time or areal forcing can allow simple analytical determinations of pressure transients in these deep porous media. Such processes indeed can have practical impacts on the CO₂ evolution for storage in deep rocks and thus influence the final site choice for a deep CO₂ injection. In synthesis, this model provides simple characterizations of thermo-poro-elastic transients for CO₂ storage.

Keywords: Injections of CO₂ and their pressure dynamics; Nonlinear thermo-poro-elastic pressure transients in fluid saturated porous media; Application to CO₂ storage and sequestration

1. The problem

Among the major challenges in mitigating climate change effects is the reduction of the CO₂ percentage in the atmosphere, which would lead to a stabilization of the today planet CO₂ concentration hopefully to be less than ≈ 550 ppm i.e., twice the pre-industrial level. In more detail, the geological storage and/or sequestration of CO₂ is a particularly important option for significant reductions of the carbon emissions into the planet atmosphere. Carbon dioxide sequestration in geological media can indeed be analyzed by many different approaches, as the analysis of geological stratigraphic and structural trapping in old oil and gas reservoirs, in solubility trapping res-

ervoirs of oil, in formation water, in adsorption trapping in un-economic beds and mainly in cavern trapping, in salt structures or by mineral immobilization [Gunter et al., 1998].

In addition, these rocks must have the porosity and permeability necessary for a CO₂, to prevent or at least to delay any CO₂ return to the atmosphere for geologically significant times [Hasanvand et al., 2013; Cheng, 2013]. Crystalline and metamorphic rocks as granite or clay therefore are not suitable for a CO₂ storage or sequestration, due to their fractured nature and their low permeability and porosity.

We here discuss general solutions of a 1-*D* analytic nonlinear model of pressure *P* and temperature *T* in fluid saturated porous rocks, following a remark by Rice and Cleary [1976] that the local energy must have both kinetic and thermal components. In short, we here consider the dynamics of an analytic nonlinear *P* model that are dealing with nonlinear convection, fluid-rock frictions and thermal effects.

We moreover briefly discuss the effects due to the evolution of heat exchanges with the neighboring rocks, or eventual local parameter variations. On the other hand, we here give no particular attention to such CO₂ seen in form of gas, or as a compressible fluid nor in our model equations is considered the CO₂ compressibility. Indeed, the factor of compressibility *Z* of CO₂ in the temperature range 20°C-100°C and pressure range 1-13 MPa is always less than 1 (0.13 < *Z* < 0.97). This implies that CO₂ is more compressible than an ideal gas and, therefore, incompressibility is not expected for CO₂ injection in wells and successive diffusion in rocks of carbon dioxide at the above defined *P* and *T* conditions. Obviously, this conclusion holds if no exchanges between CO₂ and rocks or brine occur at depth.

2. Early analyses

The CO₂ dynamics in fluid-saturated porous rocks has been already analyzed by computational mathematics [Elenius and Johannsen, 2012], simulations of density driven convection [Cheng, 2013, Cheng and Zang, 2010], wave analyses of two phases flows [Lambert et al., 2019] among others. We also note that in modeling CO₂ storage, complex numerical computations are often used [Celia et al., 2015, Andersen and Nielsen, 2018, among others].

We thus focus on a nonlinear 1-*D* analytic model, considering nonlinear fluid-rock frictions and thermal convection, which could be of interest focusing on the deep pressure dynamics in fluid saturated porous rocks. Indeed, following a remark by Rice and Cleary [1976] we discuss the solutions of a 1-*D* analytic nonlinear model of pressure *P* and temperature *T* in fluid saturated porous rocks.

In more detail we consider the dynamics of 1-*D* transients of *P* from a fluid saturated homogeneous “source” rock, with initial pressure *P*₀ + *P*_{*I*} as Salusti et al. [2019], and an asymptotic porous medium with a pressure *P*₀ and describe their effects on such CO₂ injections. In early studies [McTigue, 1986; Bonafede, 1991; Merlani et al., 2001, 2015; Caserta et al., 2017; Garra et al., 2015] and coworkers examined 1-*D* models of such transients. In particular, a 1-*D* choice can be valid for a radial transient or from cylindrical perforated segment of a borehole thus forming a segment source, or also for a two half-horizon schematization.

About these problems, Mc Tigue [1986] discussed a *P-T* interaction (Appendix A) as

$$\frac{\partial P}{\partial t} = B \frac{\partial^2 P}{\partial x^2} + C \frac{\partial^2 T}{\partial x^2} + A \frac{\partial T}{\partial t} \quad (1)$$

where *A*, *B*, *C* are functions of geological properties and their physical dimensions in Mc Tigue [1986] and in SI are:

$$A = \frac{2GBb^{*2}(1+\nu^*)(1+\nu_u^*)}{9(\nu_u^*-\nu^*)}(\alpha_f - \alpha_m) \approx 10^5, \quad B = \frac{2kG}{\mu} \left[\frac{b^{*2}(1-\nu^*)(1+\nu^*)^2}{9(1-\nu_u^*)(\nu_u^*-\nu^*)} \right] \approx 0,1, \quad C = \frac{4GBb^*(1+\nu^*)\alpha_m}{9(1-\nu_u^*)} \approx 10^4$$

and where $u = -\frac{k}{\mu} \frac{\partial P}{\partial x}$ is the Darcy velocity, the porosity is ϕ , the medium permeability is *k*, μ is the fluid viscosity parameter, *G* is the shear modulus, the drained Poisson ratio is ν^* , the untrained Poisson ratio is ν_u^* , $\alpha_m(\alpha_f)$ is the volumetric thermal expansion coefficient for the solid (fluid) and *b*^{*} is the Skempton parameter.

3. The energy conservation equation

Following the above remark [Rice and Cleary 1976], for small velocities one can focus on the classical equation of thermal energy conservation [Bonafede, 1991]

$$\frac{\partial T}{\partial t} = E \frac{\partial^2 T}{\partial x^2} + X \frac{\partial P}{\partial x} \frac{\partial T}{\partial x} + Y' \left(\frac{\partial P}{\partial x} \right)^2 \quad (2)$$

where in SI the diffusion coefficient is $E = \frac{K_T}{\phi \rho_f c_f + (1 - \phi) \rho_m c_m} \approx 10^{-6}$, the convection coefficient is

$$X = \frac{k \rho_f c_f}{\mu [\phi \rho_f c_f + (1 - \phi) \rho_m c_m]} \approx 10^{-12}, \quad \text{and} \quad \text{the fluid-rock friction coefficient is}$$

$$Y' = \frac{k}{\mu [\rho_f c_f + (1 - \phi) \rho_m c_m]} \approx 10^{-17}. \quad \text{Here } K_T \text{ is the thermal conductivity, } \rho_m \text{ is the rock density, } c_f \text{ and } c_m \text{ are}$$

the fluid and rock heat capacities, discussed in our final Table 1. We stress that are these geologic properties that play the dynamical roles. In addition, we note how in equation (2) is considered the nonlinear convection with coefficient X , and fluid-rock ‘‘friction’’ with a novel coefficient Y' discussed in the Appendix B.

Parameter	Abyssal Red Clay	Berea sandstone	Ruhr sandstone	Weber sandstone	Westerly granite
B	$2 \cdot 10^{-8}$	0.5	0.0004	0.002	10^{-4}
E	$2 \cdot 10^{-7}$	$3 \cdot 10^{-6}$	10^{-6}	$2 \cdot 10^{-6}$	$2 \cdot 10^{-6}$
C	$8 \cdot 10^{-7}$	$6 \cdot 10^5$	10^4	$3 \cdot 10^3$	10^3
A	$2 \cdot 10^2$	$2 \cdot 10^6$	10^6	$7 \cdot 10^6$	$6 \cdot 10^5$
X	$4 \cdot 10^{15}$	$5 \cdot 10^{11}$	$7 \cdot 10^{15}$	10^{14}	$4 \cdot 10^{20}$

Table 1. Material properties of some of the considered rocks in SI. The fluid saturated Abyssal Red Clay data have been estimated in McTigue [1986], the Berea sandstone and Ruhr sandstone are from Bonafede [1991]. The values of the other rocks are from fracturing experiments [Salusti et al. 2019]. Considering however the difficulty of estimating these rock properties in situ, we give only the orders of magnitude of the above quantities where the field uncertainties can be rather large.

4. The properties of the model solutions

About the solutions of the equations (1) and (2), [Merlani et al., 2011] and dr. Decio Levi (personal communication, 2018) suggest a simple *ansatz*, that the solutions of T and P are proportional to x^2/t in equations (1) and (2), a property to be checked in the following. From this *ansatz* and equation (1), one obtains a strict relation between P , T and the parameter A as

$$P(x, t) = A T(x, t) + f(t). \quad (3)$$

where $f(t)$ is discussed in the following. This implies that also a thermal transient strictly corresponds to a pressure transient. In addition, from the equations (1)-(3) we obtain a classical nonlinear Burgers equation for $t > \varepsilon$, as

$$\frac{\partial P}{\partial t} = E \frac{\partial^2 P}{\partial x^2} + (YA + X) \left(\frac{\partial P}{\partial x} \right)^2 = E \frac{\partial^2 P}{\partial x^2} + \Lambda \left(\frac{\partial P}{\partial x} \right)^2, \quad (4)$$

where a short time delay ε can be due to chemical effects, or to a flux of thin sands a kind of filter cake [Civan, 1998]. Moreover, this ε avoids mathematical pathologies in short-time phenomena. Equation (4) is a model of P transient dynamics at a distance x from the CO_2 injection well. We remark how $\Lambda = YA + X$, related to the fluid-rock nonlinear convection and to the “frictions” among rocks deformations or fracturing, is the basic parameter for such flow evolutions. In more detail, for a small Y this Λ is small and positive, while for a large Y it can be negative, as discussed in the Appendix C.

It is of interest that Whitham [1974] analyzes the equation (4) and defines a number

$$R = \frac{(YA + X)P}{E} = \frac{\Lambda P}{E} \quad (5)$$

i.e., the ratio of nonlinear terms over the diffusive terms. This R characterizes a linear pressure diffusion for $R < 8-10$, while for $R > 8-10$ the solution is a sharp and quick impulse (Figure 1). In addition, a scale analysis in the Appendix D shows that the effects of the diffusion in equation (5) are small about 1/100 times than these of the nonlinear terms.

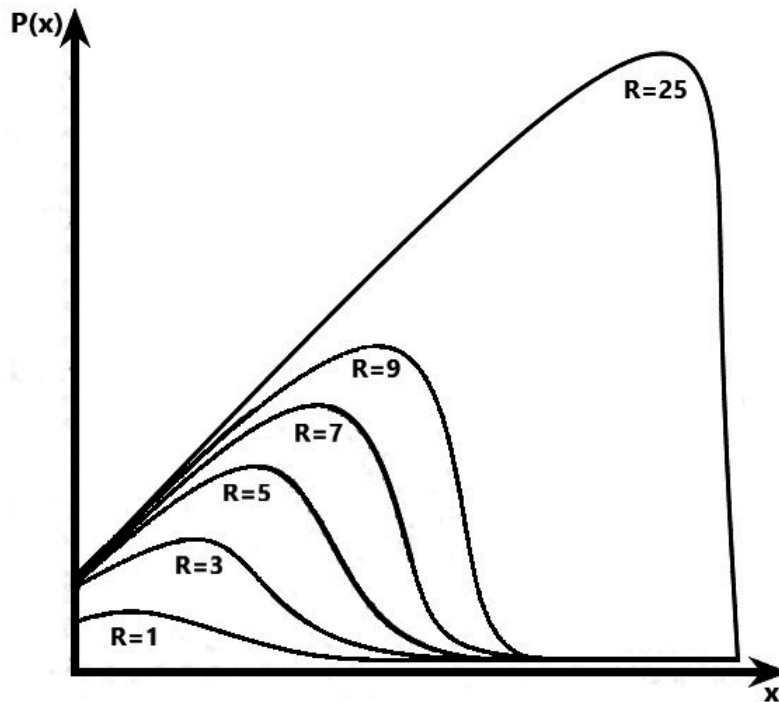


Figure 1. Sketch for the solutions of the Burgers equation for various values of R .

5. Solutions of the model

The solution of P transients from the “source” rock injection, with the above initial pressure $P = P_0 + P_I$, and P_0 for a large x as in Salusti et al. [2019], for $t > \varepsilon$ and a positive Λ are

$$\begin{aligned} P(x, t) &= P_0 + P_I & 0 < x; t < 0 \\ P(x, t) &\approx P_0 + P_I - \frac{x^2}{4\Lambda t} & 0 < x; t > 0 \\ P(x, t) &\approx P_0 & \text{for large } x \text{ and } t \end{aligned} \quad (6)$$

For a positive Λ , these solutions are smaller for increasing distance x from the injection well (Figure 1), in agreement with general observations and also among some Zhaoxu et al. [2019] data. For a negative Y we also have similar relations, sketched in the two panels of Figure 2. A comparison of data and model is very complex, due to the many data now measured but one can compare the model result and some of the Zhaoxu et al. [2019] data.

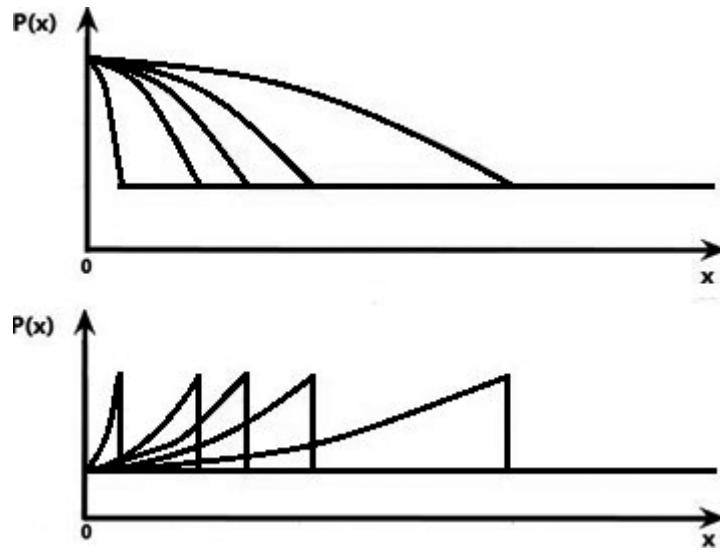


Figure 2. Intuitive sketch of the solutions for increasing times, for positive and negative parameters $X + A Y$, respectively.

6. Practical applications of the novel model solution

The equations (4) and (6) also have simple applications to particularly interesting cases:

- the solutions of (6) correspond to the above *ansatz* since the solutions are mere functions of x^2/t with a relative uncertainties about 10^{-2} , as discussed in Appendix D;
- the equation (3) allows to compute T from the pressures P , then from pressure data one can consider thermal data;
- in this complex situation about depths, places and properties of different rocks, if the CO₂ were rather slowly injected with a temperature different from that of the aquifer, a resulting novel forcing $N(t)$ can also give time dependent front expansion [Andersen and Nielsen, 2018];
- an eventual novel front, and the corresponding P , imply other interesting solutions of equation (6). Indeed, if the rock pressure receives a novel forcing $N(t)$, function of the time only, the resulting pressure evolution can be described by a simple

$$\frac{\partial P}{\partial t} = (YA + X) \left(\frac{\partial P}{\partial x} \right)^2 + N(t), \quad (7)$$

namely a forced Burgers equation, with simple solutions (Appendix D);

- e) all of this suggests to consider that a density difference between the injected CO₂ and the brine may lead to a buoyant segregation then making reasonable an assumption of vertical equilibrium [Celia et al., 2015] eventually seen as the discussed case of another external forcing;
- f) In general, if the natural pressure has a further space-dependent forcing $S(x)$, the resulting novel evolution equation for as well $E = 0$ will be

$$\frac{\partial P}{\partial t} = (YA + X) \left(\frac{\partial P}{\partial x} \right)^2 + S(x), \quad (9)$$

discussed in the Appendix D;

- g) Karsten Pruess et al. [2011] moreover discuss how from a geologic storage reservoir some fluids can migrate towards the land surface passing through lost faults, or fractures and abandoned wells. These fluids then could reach sub-critical conditions at depths shallower than 500-750 m. At this level, and at shallower depths, a subcritical CO₂ can form a two-phase mixtures of liquid and gaseous CO₂, with significant latent heat effects during boiling and condensation. And thus, we can eventually generalize the above discussed evolutions. In such complex situations one has also to consider the geological media characterizations. The sedimentary basins, where CO₂ storage most often occurs while the sandstone is the dominant rock, generally do not have natural fractures allowing perturbations of the general pressure. In contrast, about the crystalline rocks where a volcanic or seismic activity can have occurred, these rocks can have natural fractures, eventually causing remarkable pressure perturbations. Then also from such phenomena one can have critical dynamical effects on the actual CO₂ injections;
- h) In turn the mere CO₂ injection can be also seen as an external, strongly localized forcing characterized as a very strict exponential

$$\frac{\partial P}{\partial t} = (YA + X) \left(\frac{\partial P}{\partial x} \right)^2 + ae^{-[m(x-x_0)]}, \quad (10)$$

for suitable a, x_0, m , again discussed in Appendix D. Thus, we stress that in this way one could enlarge the model applications to other natural rock characteristics, or also in further x -dependent phenomena.

7. Applications to some rock examples

We now apply these model results, to check nonlinear effects of CO₂ transients in sandstones, the typical rocks of the sedimentary basins, often used for CO₂ storage and sequestration. In addition, although clay and crystalline rocks are not suitable for a CO₂ storage/sequestration, for a comparison we sketch the above applications also for these rocks. We thus very quickly describe such rock properties, while due to measurement difficulties we focus only on the order of magnitude of these thermo-poro-elastic parameters.

Berea Sandstone. This rock of fine-grained sandstone consists of quartz (70%), polycrystalline quartzose rock fragments (25%), and feldspar (5%). Its A is about $2 \cdot 10^6$ and $X \approx 5 \cdot 10^{11}$ in SI.

Weber Sandstone. This sandstone is originated from fluvial deposits, derived from an ancestral Uplift. Its sarkosic lithofacies act as permeability barriers being either cross-laminated or massively bedded. Their $A \approx 7 \cdot 10^6$ and $X \approx 10^{14}$ in SI.

Ruhr Sandstone. This rock is similar to other basins in Europe and North America. These sedimentary rock sequences were deposited during early tropical, humid climate coastal plains in an equatorial region. Its $A \approx 10^6$ and $X \approx 7 \cdot 10^{15}$ in SI.

Charcoal Granite. This rock in St. Cloud, Minnesota has a massive, dark brown to dark colors. It is among the most ancient known rocks... as the protruding parts of a paleo-structure. Thus, their $A \approx 6 \cdot 10^5$ and $X \approx 4 \cdot 10^{20}$ are particularly larger than those of the above rocks.

Abysal Red Clay. These deposits, allogenic in origin, are mostly due to rather ancient Asian aeolian dust. These particular red clays are about the 90%, then are Mn, Co, Ni and Cu of autogenic origin [Glasby, 2010]. Its $A \approx 2 \cdot 10^2$ and $X \approx 4 \cdot 10^{15}$ in SI, are rather similar to these of sandstones.

Here, we strongly emphasize the need for further field measurements of the thermo-poro-elastic properties in such deep rocks, in order to obtain more data sets also for applications of eventual novel models, for discussing future models.

8. Discussions and conclusions

Although today many approaches are used to model CO₂ storage, often also including complex numerical computations, we discuss here a simple nonlinear analytical model, a generalization of Garra et al [2015]. This model describes a theoretical approach to many hydrologic processes, showing how the deep fluid pressure solutions of such model finally are functions of

$$P(x, t) \approx P_0 + P_1 - \frac{x^2}{4\Lambda t} \quad (11)$$

for suitable parameters Λ, P_0, P_1 . Thus, our equation (11) describes the dynamics of processes dealing with different rock temperatures, pressure evolutions and their dynamic consequences. In addition, this allows one to compare critically the results of eventual numerical computations about storage/sequestration of CO₂ sites, that we now can address also with the results of this nonlinear analytic model.

It is also important that we show how eventual external temporal forcing $S(t)$, or space forcing $Q(x)$, can perturb these dynamics. Indeed, we here show that for such $S(t)$ or $Q(x)$ one can again have simple model solutions.

In addition, all of this can also be relevant to other practical applications such as for elevate or low temperature liquid storages, or also disposal of dangerous waste in porous media [Mc Tigue, 1986]. Thus, the broad implication of such novel analytic model is that it provides simple, general assessments for dynamics of thermo-poro-elastic transients, also for other applications dealing with the geological reservoir and for the realistic site selections for these or similar problems.

Appendices

Appendix A. Other similar models in the literature

The equation (1) is not the only equation of this type discussed in the literature. [Bonafede and Mazzanti, 1997] indeed assume $C = 0$ in equation (1) and Shapiro and Dinske [2009], and coworkers, analyze an interesting similar nonlinear model as

$$\left(\frac{\partial}{\partial t} - \frac{\partial}{\partial x} H(P) \frac{\partial}{\partial x}\right) P = 0 \quad (11)$$

Appendix B. Effects of nonlinear terms

We remark that the equation (2) is the classical equation of energy-heat conservation, with the nonlinear fluid “convection” $u \frac{\partial}{\partial x} T$ and the “work rate” $-\frac{k}{\mu} \left(\frac{\partial}{\partial x} P\right)^2$ in SI, here considered for rather mild dynamics. For larger effects, as rock deformations or fractures [Phillips et al., 2013; Detournay and Garagash, 2003] one can consider a different approach $Y \left(\frac{\partial}{\partial x} P\right)^2$ with an unknown Y . In more detail, the work made by the fluid pressure increases the rock temperature, and for moderate perturbations one indeed has a positive $Y' \approx k/\mu \approx 10^{-12}$ in SI [Bonafede et al., 1991]. On the other hand, rock deformations or fractures, caused by relevant perturbations, can extract from the rock some heat Φ and then one can have an energy loss for a rather large Φ as

$$X' \frac{\partial}{\partial x} P \frac{\partial}{\partial x} T - \Phi = Y' \left(\frac{\partial}{\partial x} P\right)^2 - \Phi = Y \left(\frac{\partial}{\partial x} P\right)^2 \quad (12)$$

assuming that such energy loss is somehow related to the fluid energy [Phillips et al., 2013; Detournay and Gargash, 2003]. Thus, a realistic determination of A, C, B, E, Y, Φ is not a simple challenge, and these equations must be considered critically.

Appendix C. Approximate scale analysis

As a rather rough estimate in SI, we assume for sandstones $P_l \approx 10^7, T_l \approx 10^2, A \approx 10^6, B \approx 0.1, C \approx 10^4, E \approx 10^{-6}$ and $X = 10^{13}$ for sandstones but $X \approx 10^{20}$ for granites (Table 1). From eq. (6), assuming a space scale λ and a time scale τ , for sandstones we have

$$\frac{\partial P}{\partial t} \approx \frac{10^7}{\tau}, \quad A \frac{\partial T}{\partial t} \approx \frac{10^8}{\tau}, \quad B \frac{\partial^2 P}{\partial z^2} \approx \frac{10^6}{\lambda^2}, \quad C \frac{\partial^2 T}{\partial z^2} \approx \frac{10^6}{\lambda^2} \quad (13)$$

and thus $E \frac{\partial^2 T}{\partial z^2} \approx \frac{10^{-4}}{\lambda^2}$ over $X \frac{\partial T}{\partial z} \frac{\partial P}{\partial z} \approx \frac{10^9}{\lambda^2}$ is a very small quantity. All of this confirms that the diffusive terms have smaller effects than the nonlinear terms characterized by B and C .

Appendix D. Solutions of the model equation, forced by time or space external forcing

Considering in general a forcing $N(t)$ in the Burgers equation such that

$$\frac{\partial P}{\partial t} = \left(\frac{\partial P}{\partial x} \right)^2 + N(t), \quad (14)$$

the classical solution of the Burgers equation for $N(t) = 0$ is $P = P_0 - \frac{x^2}{t}$ while for a realistic the solution is $P = P_0 - \frac{x^2}{t} + \int N(t) dt$. Considering also the scale analysis in Appendix C we here do not consider other diffusive time terms, since most probably other forcing solutions have been already studied. Indeed, the Burgers equation has been deeply examined by mathematicians and similar discussions holds also for another $M(x)$ case.

References

- Andersen, O. and H. M. Nilsen (2018). Investigating simplified modeling choices for numerical simulation of CO₂ storage with thermal effects, *Int. J. Greenh. Gas Control.*, 72, 49-64.
- Bonafede, M. (1991). Hot fluid migration: an efficient source of ground deformation to the 1982-1985 crisis at Campi Flegrei-Italy, *J. Volc. Geotherm. Res.*, 48, 182-197.
- Bonafede, M. and M. Mazzanti (1997). Hot fluid migration in compressible saturated porous media, *Geoph. J. Int.*, 128, 383-398.
- Caserta, I., R. Kanivetsky and E. Salusti (2017). On the theory of solitons of fluid pressure and solute density in geophysics porous media with application to shales, clay and sandstone, *Pure Appl. Geophys.*, 174, 4183-4196.
- Celia, M. A., S. Bachu, J. M. Nordbotten and K. W. Bandilla (2015). Status of CO₂ storage in deep saline aquifers with emphasis on modeling approaches and practical simulations, *Water Resour. Res.*, 51, 6846-6892, doi:10.1002/2015WR017609, 2015.
- Chang, F. (1998). Practical model for chemically induced formation damage, *J. Petrol. Sci. Eng.*, 17, 123-137.
- Cheng, C. and D. Zang (2010). Pore-scale simulation of density driven convection in fractured porous media during geological CO₂ sequestration. *Water Resour. Res.*, 46.
- Civan, F. (1998). Incompressible cake filtration: mechanism, parameters, and modeling, *AICHE J.* 44 (11), 2379-2387.

- Detournay, E. and D. Garagash (2003). The tip region of a fluid-driven fracture in a permeable elastic solid, *J. Fluid Mech.* 494, 1-32.
- Elenius, M.T. and K. Johannsen (2012). On the time scales of nonlinear instability in immiscible displacement porous media flow, *Computational Geoscience*. doi: 10.1007/s10596-012-9294-2.
- Garra, R., E. Salusti and R. Droghei (2015). Memory effects on nonlinear temperature and pressure wave propagation in the boundary between two fluid-saturated porous rocks, *Advances in Mathematical Physics*, 6, doi: 10.1155/2015/532150.
- Glasby, G.P. (2010). Mineralogy, geochemistry, and origin of Pacific red clays: a review, *New Zealand J. Geol. Geophys.* 34 (2), 167-176.
- Gunter, W.D., S. Wong, D. B. Cheel and G. Sjestrom (1998). Large CO₂ Sinks: Their role in mitigation of greenhouse gases from an international, national (Canadian) and provincial (Alberta) perspective, *Applied Energy*, 61, 4.
- Hasanvand, M.Z., M.A. Ahmadi, S.R. Shadizadeh, R. Behbabani and R. Feyzi (2013). A Geological storage of carbon dioxide by injection of carbonated water in an Iranian oil reservoir: a case study, *J. Petrol. Sci. Eng.*, 111, 170-177.
- Karsten Pruess et al. (2011). Integrated Modeling of CO₂ Storage and Leakage Scenarios Including Transitions between Super- and Sub-Critical Conditions, and Phase Change between Liquid and Gaseous CO₂, *Earth Sciences Division, Lawrence Berkeley National Laboratory University of California, Berkeley, CA 94720, USA*
- Lambert, W. J., A.C. Alvarez, V. Matos, D. Marchesin, and J. Bruining (2019). Nonlinear wave analysis of geochemical injection for multicomponent two phases flow in porous media, *Journal of Differential Equations*, 266(1), 406-454.
- McTigue, D.F. (1986). Thermoelastic response of fluid-saturated rock, *J. Geophys. Research*, 91, 9533-9542.
- Merlani, A.L., G. Natale and E. Salusti (2001). Fracturing processes due to nonlinear shock waves propagating in fluid-saturated porous rocks, *J. Geophys. Research*, 106, 6.
- Merlani, A. L., E. Salusti and G. Violini (2011). Non-linear waves of fluid pressure and contaminant density in swelling shales, *Journal of Petroleum Science and Engineering*, 79, 1-9.
- Philips, S. L., F. Afsar and E. Gudmundsson (2013). Effects of mechanical layering on hydrofracture emplacement and fluid transport in reservoirs, *Frontiers of Earth science*.
- Rice, J.R., and M. P. Cleary (1976). Some basic stress-diffusion solutions for fluid saturated elastic media with compressible constituents, *Rev. Geophys. Space Phys.*, 14, 227- 241.
- Rice, J.R. (2006). Heating and weakening of faults during earthquake slip, *J. Geophys. Res.*, 111 (B5), B05311, 29.
- Salusti, E., R. Kanivetsky, R. Droghei and R. Garra (2019). On the propagation of nonlinear transients of temperature and pore pressure in a thin porous boundary layer between two rocks, *Journal of Hydrology*, 576, 520-527.
- Shapiro, S. and C. Dinske (2009). Fluid-induced seismicity: Pressure diffusion and hydraulic fracturing. *Geophysical Prospecting*, 57, 301-310.
- Whitham G.B., *Linear and Nonlinear Waves*, Wiley, New York (1974).
- Zhaoyang, L. J. and L. J. Durlofsky (2015). Reduced-order modeling of CO₂ storage operations, *J. Greenh. Gas Control.*, 68, 49-67.
- Zencher, F., M. Bonafede and R. Stefansson (2006). Near-lithostatic pore pressure at seismogenic depths: a thermo-poro-elastic model, *Geophys. J. Int.*, 166, 1318-1334.
- Zhaoxu M., F. Wang, Z. Yang, X. Li, Y. Diao, X. Ma and H. Tian (2019). Numerical Simulation of the Influence of Geological CO₂ Storage on the Hydrodynamic Field of a Reservoir *Geofluids*, Article ID 1853274, <https://doi.org/10.1155/2019/1853274>.